OAK RIDGE NATIONAL LABORATORY LIBRARIES
3 4456 0550241 7

CENTRAL RESEARCH LIBRARY

ORNL-TM-4536

Cy 26

ISOTOPIC POWER MATERIALS DEVELOPMENT PROGRESS REPORT FOR FEBRUARY 1974

R. G. Donnelly

[redacted]

OAK RIDGE NATIONAL LABORATORY
CENTRAL RESEARCH LIBRARY
DOCUMENT COLLECTION
LIBRARY LOAN COPY
DO NOT TRANSFER TO ANOTHER PERSON
If you wish someone else to see this document, send in name with document and the library will arrange a loan.
UCN-7969
(3 3-67)

OAK RIDGE NATIONAL LABORATORY
OPERATED BY UNION CARBIDE CORPORATION • FOR THE U.S. ATOMIC ENERGY COMMISSION

This report was prepared as an account of work sponsored by the United States Government. Neither the United States nor the United States Atomic Energy Commission, nor any of their employees, nor any of their contractors, subcontractors, or their employees, makes any warranty, express or implied, or assumes any legal liability or responsibility for the accuracy, completeness or usefulness of any information, apparatus, product or process disclosed, or represents that its use would not infringe privately owned rights.

ORNL-TM-4536

Contract No. W-7405-eng-26

METALS AND CERAMICS DIVISION

ISOTOPIC POWER MATERIALS DEVELOPMENT PROGRESS REPORT FOR FEBRUARY 1974

R. G. Donnelly

MAY 1974

NOTICE This document contains information of a preliminary nature and was prepared primarily for internal use at the Oak Ridge National Laboratory. It is subject to revision or correction and therefore does not represent a final report.

OAK RIDGE NATIONAL LABORATORY
Oak Ridge, Tennessee 37830
operated by
UNION CARBIDE CORPORATION
for the
U.S. ATOMIC ENERGY COMMISSION

OAK RIDGE NATIONAL LABORATORY LIBRARIES

3 4456 0550241 7

CONTENTS

Page

IRIDIUM FABRICATION PROGRAM 1
Fabrication of Iridium for PICS 1
Production of Blanks (PICS) 1
Recrystallization of Ir–0.3% W Sheet 3
Fabrication of Iridium Cylinders 5
Multipiece Cylinder Sheet Rolling and Forming 6
Multipiece Cylinder Welding Development 8
Single-Piece Cylinder Ingot Preparation and Breakdown . . . 10
Fabrication of End Caps for Outer Clad 11
Sheet Rolling 12
HIGH-TEMPERATURE ALLOYS FOR SPACE ISOTOPIC HEAT SOURCES 13
Development of Iridium Alloys 13
Tensile Properties 13
Air Oxidation 14
Thermomechanical Effects on Iridium-Tungsten Alloys 14
Evaluation of Impact Behavior of PICS 15
Ruthenium Characterization and Fabrication Development 21
Platinum-Rhodium-Tungsten Alloys 21
CURIUM-244 FUEL DEVELOPMENT 25
Compatibility Testing 25
FY-1973 Compatibility Matrix 25
FY-1974 Compatibility Matrix 25

IRIDIUM FABRICATION PROGRAM

Fabrication of Iridium for PICS

A. C. Schaffhauser

Production of Ir–0.3% W forming blanks for the MHW post-impact containment shells (PICS) has continued. The higher recrystallization temperature and hardness of sheet fabricated from the WE batch of iridium powder required a 100°C increase in our processing temperatures to meet specifications and improve material yield. Experimental arc-melted ingots were also fabricated at the higher temperatures.

The status of materials in process and blanks shipped during the month is given in Table 1. An additional 150 square inches of 0.005-in. Ir–0.3% W foil was fabricated and delivered to Mound Laboratory this month.

Table 1. Status of Material for Forming Blanks (February 28, 1974)

Batch Designation	Material Completed for Each Fabrication Step During February					Number of Blanks Shipped	Cumulative Total Shipped FY 1974
	Compacts Produced (g)	Ingots Melted[a]	Sheets Rolled[a]	Blanks Machined[a]	Blanks Shipped[a]		
WE	15,002	34–63	28–57	16–51	10–39	84	222
AM[b]	--	F1,D1[b]	F1,D1[b]	--	--	--	--
Ir–2% W	--	--	--	6	--	--	--
Ir–2% Re	--	--	--	6	--	--	--

[a]Ingot, sheet, or blank number.

[b]Arc melted; F – finger, D – drop casting.

Production of Blanks (PICS) – (D. N. Braski)

Sheets of Ir–0.3% W produced from the WE lot of powder have demonstrated somewhat higher mechanical properties than those fabricated from WC-series material (see "Evaluation of Impact Behavior of PICS," p. 15, this report). In addition, recrystallization temperatures measured on

WE-series sheet were approximately 100°C higher than previously processed iridium sheet.[1] At the same time, these differences in properties were reflected in the production line by a definite increase in the hardness of the Ir–0.3% W sheet during rolling and an increase in surface roughness of the final sheet from which blanks were machined. Photomicrographs of the longitudinal section from WE-sheet showed a relatively coarse, fibrous microstructure with some large stringers or elongated grains, indicating that the original cast structure had not been sufficiently broken down during warm rolling. Microhardness values of these sheet fell near the upper limit of the specification and were higher than those measured for WC-series sheet. A 25 to 30% reduction in production yield of WE-series iridium blanks resulted due to the inability to achieve good cleanup of the blank surfaces during grinding. A number of WE-blanks also failed to pass the ultrasonic inspection. These problems were virtually eliminated by making the following changes to the warm-rolling procedures:

1. Rolling and annealing temperatures were increased by 100°C.
2. The iridium sheet was bare rolled (no cover sheets) from a 0.040 to a 0.033-in.-thickness at 1050°C.
3. The final stress-relief-anneal temperature was increased to 950°C.

All WE-series blanks with numbers of 40 or greater were fabricated using the above process changes. These later WE-series blanks possessed a fine fibrous microstructure with little or no recrystallized grains present, an optimum microstructure for hydroforming.

Another problem associated with the WE-series blanks was the increasing number of visual surface indications that were being reported by NDT. Although the blanks with visual indications were within specification, they contained surface scratches with depths of 0.3 to 1.0 mils, as measured with a calibrated metallograph. The surface scratches were introduced during the surface grinding process. These scratches did not show as dye-penetrant indications.

---

[1]R. G. Donnelly, Isotopic Power Materials Development Progress Report for January 1974, ORNL-TM-4535 (to be published).

In an attempt to improve the surface finish, a grinding wheel having a finer grit size was used in a trial run to grind the WE-50 blanks. The results were successful, and all subsequent blanks have been ground using this wheel. Table 2 shows the percentage of blanks shipped having visual surface indications for each type of grinding wheel.

Table 2. Correlation of Surface Indications with Type of Grinding Wheel Used

Blank Number	Grinding Wheel Grit Size	Total Shipped	Number of Surface Indications	Percentage of Blanks with Surface Indications
WE-40–49	Medium	36	33	92
WE-50–57	Fine	29	10	35
WE-58–63	Fine	19	1	5

A summary of data on blanks shipped during the month is given in Table 3.

Recrystallization of Ir–0.3% W Sheet – (D. N. Braski)

The results of additional recrystallization studies conducted on the WE-series material are given in Table 4. Data for WC series sheet are also included for comparison. All samples were annealed 15 min, withdrawn from the furnace, and then air cooled to room temperature. The percent of recrystallization was estimated by metallographic examination of the samples. The hardness values shown are the average of five readings taken across a particular sample. Several important conclusions may be drawn from the recrystallization results. First, the WE-series material recrystallizes nearly 150°C higher than WC-series material for which the fabrication parameters were set. These parameters have been adjusted for the WE material as described in the section on PICS production. Secondly, recrystallization data taken from a later lot of WE sheet, WE-22, indicates that the recrystallization behavior was constant within this batch of material. This result is important in that the factors such as ingot chemistry, which have caused the difference in

Table 3. Disposition and Characteristics of Ir–0.3% W Blanks

Ingot Number	Number Manufactured	Nonconformance and Notes			Number Shipped	Average Hardness (DPH)	Tungsten Content (ppm)
		Ultrasonic	Penetrant	Surface			
WE-11	4	1[a]	0	1[a,b]	2	520	3100
WE-12	4	1[c]	0	1[b]	4	514	3200
WE-13	3	0	0	0	3	480	3000
WE-14	4	0	0	1[a,b]	3	544	2800
WE-15	4	0	0	3[b]	4	542	3000
WE-16	4	0	0	0	4	530	3000
WE-17	4	1[a]	0	0	3	559	2500
WE-18	4	0	0	3[b]	4	521	2500
WE-21	4	2[c]	1[c]	1[b]	4	573	3000
WE-22	4	2[c], 1[a]	0	1[b]	3	542	3400
WE-23	1	1[a]	0	0	0	-	--
WE-24	4	0	0	3[b]	4	531	4000
WE-25	4	2[a], 1[c]	0	0	2	544	2600
WE-26	4	2[a]	0	0	2	596	3800
WE-28	4	0	0	0	4	537	2800
WE-29	3	0	0	0	3	534	3400
WE-30	4	0	0	0	4	501	3000
WE-31	3	1[a]	0	0	2	540	2800
WE-32	3	2[a]	0	0	1	521	2800
WE-33	3	0	0	0	3	513	2700
WE-34	4	0	0	0	4	527	3500
WE-35	4	1[a]	0	0	3	549	3500
WE-36	4	1[a]	1[a]	0	2	512	4000
WE-37	3	0	0	0	3	468	3500
WE-38	4	0	0	0	4	455	3900
WE-39	4	0	0	0	4	456	3000
* 4	3	0	0	0	3	515	3400
* 5	1	0	0	0	1	516	3000
* 7	1	0	0	0	1	520	3500

*Samples held for rework and later shipped. [a]Rejection. [b]Visual notes, conform to specification.

[c]Borderline to specification; shipped to MRC for further evaluation.

Table 4. Recrystallization Data for Ir–0.3% W Sheet

Annealing Temperature (°C)	Recrystallization (%)	Average Hardness (DPH)
	WE-1	
800	0	573.6
850	0	573.8
900	0	557.1
950	0	561.1
1000	0.5	580.6
1050	0.5	532.1
1100	15	467.1
1150	75	301.6
1200	100	272.2
	WE-22	
1100	40	470.5
1150	86	335.1
1200	98	267.9
	WC-61	
800	3	578.8
850	4	591.6
900	4	550.6
950	7	553.8
1000	60	453.2
1050	96	274.8

recrystallization behavior between WC and WE material, are remaining constant through the WE series. Further studies are now under way to ascertain whether the change in processing variables has affected the recrystallization behavior of WE-series sheet (i.e., all WE sheet produced after WE-39).

Fabrication of Iridium Cylinders

A. J. Moorhead

Work has continued on the development of procedures for fabrication of the cylindrical portion of the outer clad of the MHW heat source. Two separate approaches are being undertaken: (1) a multipiece cylinder

made up of three or more 0.010-in.-thick tube segments and two 0.030-in.-thick end rings and (2) a single-piece cylinder in which the tube portion is produced by grinding the inside of a 0.030-in.-thick tube, thus having integral end rings. The latter approach has the obvious advantage of minimizing the number of welds required (only one longitudinal seam weld joining 0.030-in.-thick sheet), but requires the development of capabilities for fabricating large sheets of iridium and for grinding the formed and welded tube. The multipiece approach has the advantage that "small" segments should be easier to fabricate but the disadvantage of requiring welds joining 0.010- to 0.010-in.-thick sheet, 0.030- to 0.030-in.-thick sheet, and 0.010- to 0.030-in.-thick sheet. The identification and status of materials in process are given in Table 5.

Table 5. Status of Materials in Process for MHW Outer Clad Cylinders (February 28, 1974)

Item	Ingot Number	Status
First Multipiece Cylinder	WD-6/8, 9/10, 11/12, 13/14, 15/16, WCR-98	Tube section welded, but closure weld resulted in buckling in weld area
End Rings	WD-17, 18, WCR-97	Rolled to 0.030 in. sheet, trimmed, formed, and one ring welded
Lugs		Rolled to 0.104 in. and formed
Second Multipiece Cylinder	WF-1 through WF-9	Ingots have been cast
First One-Piece Cylinder	OC-2	Ingot has been rolled to 0.040 in.; now preparing for final roll to 0.030 in.
Second One-Piece Cylinder	OC-4	Ingot has been melted and trimmed; awaiting moly frame

Multipiece Cylinder Sheet Rolling and Forming – (R. W. Knight and A. C. Schaffhauser)

Sheet stock for a multipiece cylinder was rolled using double-wide ingots WD 6-8, 9-10, 11-12, 13-14, and 15-16. The double width was achieved by electron-beam welding two standard 3/4 × 3/4 × 2 in. ingots

together. After welding, the ingots were radiographed for defects and heat treated at 1500°C for 4 hr. The initial rolling schedule was the same as that used for rolling sheet for PICS blanks except that the sheet was 0.035 to 0.040 in. thick. At this point it was removed from the frame and cover and bare rolled at 950°C to smooth the surface. The sheets were final rolled in Inconel 600 at 800°C to approximately 0.010 in. thick by 8 in. wide by 18 in. long.

Sheet WD 6-8 had a weld defect and was cut into two strips. WD 9-10 failed during rolling and was cut to 7 × 12 in. for welding development. WD 11-12 and subsequent sheets were given an intermediate trim to maintain better edge and length control during the 800°C rolling in Inconel. Sheets WD 13-14 and 15-16 rolled very well, producing panels 7 1/2 × 16 × 0.010 in. The sheets were ultrasonically examined (using a 1/32-in.-diam × 0.005-in.-deep standard) and showed no defects.

Sheet WD 11-12 was formed using a marforming roller and a three-roll bender. This procedure was moderately successful, but it was obvious that a final hot forming step would be required. A graphite die was made for this operation. This sheet cracked in the weld zone during the forming operation and was separated into two pieces which were final hot formed at 950°C for 15 min at temperature. All subsequent forming was done on a three-roll bender after heat treating the part for 15 min at 950°C in vacuum. It was found during the second sheet forming that the segment must be overformed approximately 1 in. on the diameter to allow for relaxation during hot forming. WD 13-14 and WD 15-16 formed with no problems.

All sheets were thoroughly cleaned before each step where heat was required to reduce surface contamination. Cleaning consisted of immersion in aqua regia plus 10% HF followed by a water rinse; NaOH solutions with water rinse, KCN etch with water rinse, and a final cleaning in aqua regia plus 10% HF.

Ingot WCR-97 was rolled to 6 × 17 × 0.010 in. for a backup tube segment for the multipiece cylinder. The rolling parameters were the same as for the double-wide ingots except for deletion of the bare rolling passes. This resulted in an "orange-peel" surface finish on the final rolled sheet.

Material for three end rings was rolled from ingots WD-17 and -18 and WCR-98, which were 3/4 × 3/4 × 2 1/8 in. The rolling schedule was the same as for sheet for PICS blanks except only two cross roll passes were taken in the initial breakdown. All succeeding passes were longitudinal rolled, yielding strips 1 3/4 in. wide by 25 in. long by 0.032 in. thick. Strips were cut to 0.960 in. wide by 22.5 in. long and roll formed. The strips were overformed approximately 1/2 in. and hot sized in a graphite die at 1000°C for 1/2 hr.

Material for the lifting lugs of the cylinder was rolled to 0.104 in. thick sheet using the same rolling parameters as above. The sheet was formed to the proper curvature on a three-roll bender and sent to Y-12 for machining.

Multipiece Cylinder Welding Development – (A. J. Moorhead)

Parameters were developed on flat coupons for electron-beam welding the three major joint types required for the multipiece cylinder: (1) 0.010 to 0.010-in.-thick sheet (longitudinal seam weld of tube), (2) 0.030 to 0.030-in.-thick sheet (butt weld to form end rings), and (3) 0.030 to 0.010-in.-thick sheet (girth weld joining tube to ring). Typical parameters for each of these joints are given in Table 6.

Transverse weld shrinkage measurements across several 12-in.-long longitudinal seam welds showed this value to be 0.008 to 0.010 in. Selected weld coupons were inspected visually, with fluorescent dye penetrant, and metallographically. These examinations revealed that

Table 6. Parameters for Electron-Beam Welding Iridium Cylinder Joints

	Longitudinal Seam	Ring Butt	Ring-to-Tube
Accelerating potential, kV	100	106	100
Beam current, mA	4	10	6
Travel speed, ipm	15	18	20
Focus current, A	0.025 (defocus)	0.015 (defocus)	0.010 (defocus)

weld cracking or porosity does not seem to be significant problems in this material. However, several problem areas did arise, as follows: (1) an abrupt protrusion of some longitudinal seam welds above or below the surface, (2) burnthroughs, and (3) low-melting phases in the heat-affected zone (HAZ). Each of these conditions will be discussed separately below.

The protrusion of an occasional weld joining two 0.010-in.-thick iridium sheets has been a baffling problem. The condition is not a drop-through of the weldment, but rather appears as a ridge or depression running the full length of the weld. The protrusion appears to be limited to the weld fusion and heat-affected zone. This phenomenon appears to be related to the weld fixture, as modifications to the fixture have brought about improvements. However, this condition still occurs periodically, so that it is not yet fully understood.

Burnthroughs (small holes in the fusion zone) have occurred in over one-third of all full-length longitudinal welds. The cause of this phenomenon is not known, and it appears to occur at random. We can hypothesize that it is related to some defect in the base metal (either a delamination or lower melting particle) as the welder observes a small "explosion" whenever a burnthrough occurs. We have developed a procedure for successfully repairing burnthroughs by the manual gas tungsten-arc process using a current of about 25 A-dc. The repair is done in the open rather than in an inert atmosphere chamber for better visibility.

An occasional weld-related defect is found which appears to be due to the melting of a lower melting point particle in the HAZ. This low-melting phase apparently wets the grain boundaries, causing both fusion zone and HAZ cracking. We examined two of these areas (which occurred in weld 18) using both the scanning electron microscope and the electron microprobe (using energy dispersive x rays). One area showed a high concentration of iron and the other was high in aluminum. Apparently these were particles embedded in the sheet during fabrication which were not removed during chemical cleaning. We have subsequently added an abrasive cleaning step (320-grit paper) in the weld region just prior to welding, and this operation has reduced the number of occurrences of

this phenomenon. In cases in which it has occurred, we have successfully repaired the region by drilling out the defect and repairing as for a burnthrough.

Two test welds were made (on flat sheet) which simulated a ring-to-tube weld crossing a longitudinal seam weld. Both of these welds (Nos. 20 and 21) looked good visually and fluorescent penetrant inspection revealed no defects in the area around the crossover point. A portion of each weld has been removed for metallographic examination.

Samples of all three joints were welded on WC material which had been heat treated in vacuum for 60 min at 1050°C. The purpose was to see if there was any difference, as far as welding behavior was concerned, between the partially recrystallized material studied to date and this fully recrystallized base metal. No difference in welding behavior was observed, and fluorescent penetrant inspection revealed no defects.

Several fixtures were designed and built during this report period, including a lug proof-test fixture and a second circumferential welding fixture. The latter is to be used if the ring-to-tube joint is changed from the present GE design to one in which the ring is machined to produce a square-butt joint with the tube. Flat test coupons have been machined with the new joint design, but no welds have been made.

Single-Piece Cylinder Ingot Preparation and Breakdown — (R. W. Knight and A. C. Schaffhauser)

Sheet material for the single-piece-cylinder approach is being fabricated from electron-beam-melted ingots 4 × 4 × 1 in. in size. The first cylinder ingot, OC-2, was stress relieved at 1100°C and the edges were electron-beam weld conditioned to conserve material. The ingot was ground to 4.867 × 4.867 × about 1.050 in. thick. After grinding, the ingot was homogenized 4 hr at 1500°C. Hot rolling was done in a molybdenum frame with molybdenum cover sheets at 1300°C with three straight passes of 16.5%, 19.8%, and 18.5% reduction and four cross passes of 15.1%, 8.9%, 9.8%, and 10.9% reduction. The lighter passes were of no value, and all future reductions, insofar as possible, will be 25%, but not to exceed 0.2 in.

The ingot was removed from the frame, cleaned, and sent to weld repair to heal surface cracks. After welding, the ingot was reframed and rolling continued at 1300°C. Pass 1 was 25% longitudinal, pass 2 4% cross. and passes 3 through 6 were each 25% in the longitudinal direction. This procedure yielded an ingot 6 1/2 × 13 3/4 × about 0.150 in. thick. The ingot was removed from the frame, cleaned, and sent to the Y-12 Plant for rolling to 0.030 in. sheet.

The sheet being fabricated from ingot OC-2 has been final rolled to 17 1/2 × 24 × 0.030 in. The sheet was radiographed and dye-penetrant checked. Cracking was noted over an area about 4 × 9 in. Most of these defects appeared to be subsurface.

This sheet was trimmed to 17 × 22 × 0.031 in., flattened, and heat treated between graphite blocks at 1050°C for 1/2 hr at temperature. The sheet was then formed in two steps at room temperature on a two-roll bender. After the first step, the part was annealed for 1/2 hr at 1100°C. On completion of rolling the part was returned to ORNL for sizing in a graphite die prior to welding.

Fabrication of End Caps for Outer Clad

A. C. Schaffhauser

Material is being prepared for the fabrication of three sets of Ir–0.3% W MHW outer clad end caps. The status of these materials is given in Table 7.

Table 7. Status of Materials in Process for MHW Outer Clad End Caps (February 28, 1974)

Set	Ingot Number	Status
First	OC-1	Rolled to 0.040 in. and cut for four blanks
Second	OC-3	Ingot has been through breakdown roll and weld condition and is now ready for further rolling
Third	OC-5	Compacts for melting have been completed

Sheet Rolling – (R. W. Knight and D. S. Parker[2])

We continued fabrication of sheet OC-1 from the first electron-beam-melted pancake ingot to provide 0.030-in.-thick sheet for forming end caps. The sheet was previously rolled to 9 × 11 × 0.094 in. at ORNL. The sheet was inspected, trimmed, reframed, and covered with molybdenum, then rolled at 1100°C to 0.040-in. thickness at Y-12. The material was inspected and cut into four pieces for final rolling at ORNL. Each piece was bare rolled (no molybdenum covers) at 1100°C to 0.030-in. thickness. The sheets were rotated 90 deg each pass to obtain an 8 × 8 in. sheet. After rolling, the sheets were cleaned by KCN electroetching and acid etching as described previously. The sheets were annealed 30 min at 1000°C and returned to Y-12 for blanking and forming.

The second ingot for end caps, OC-3, required weld conditioning and grinding only on the edges. The ingot was then cleaned, homogenized 4 hr at 1500°C, framed and covered with molybdenum, and rolled at 1300°C to 0.330-in.-thick plate. The plate was cleaned, weld conditioned, homogenized, reframed, and rolled to 0.24-in.-thick sheet at 1300°C. Further rolling to 0.20-in. thickness was done bare to smooth the surface of the sheet. The sheet is being recovered at Y-12 for rolling to 0.040 in. thickness, then it will be bare rolled to 0.030 in. This sheet should yield four to five forming blanks for end caps.

---

[2]Union Carbide Corporation, Nuclear Division, Y-12 Plant, Oak Ridge, Tennessee.

HIGH-TEMPERATURE ALLOYS FOR SPACE ISOTOPIC HEAT SOURCES

H. Inouye

Development of Iridium Alloys

C. T. Liu and H. Inouye

Tensile Properties

Tensile specimens with a gage section of 1/2 × 1/8 in. were blanked from alloy sheets of Ir–8% Re, annealed 1 hr at 1500°C, and then tested in vacuum at room temperature, 760 and 1093°C. The results are presented in Table 8 together with those for other Ir-Re alloys. The strength increases with rhenium content. The alloy Ir–8% Re reaches a tensile strength of 68.8 ksi at 1093°C. The ductility of the alloys at room temperature and 760°C decreases with rhenium content above 2%.

Table 8. Tensile Properties of Ir-Re Alloy Sheets[a]

Alloy (wt %)	Strength, ksi		Elongation (%)
	Yield	Tensile	
	Room Temperature		
Ir (EBP-21)	7.2	48.0	14.1
Ir–1 Re	25.5	48.0	6.6
Ir–1.98 Re	26.0	67.6	8.9
Ir–3.96 Re	32.1	60.6	6.4
Ir–8 Re	48.6	59.9	4.2
	760°C		
Ir (EBP-21)	8.2	56.9	38.4
Ir–1 Re	22.0	50.0	20.0
Ir–1.98 Re	19.3	67.3	28.0
Ir–3.96 Re	23.1	70.2	20.0
Ir–8 Re	27.1	62.8	12.5
	1093°C		
Ir (EBP-21)	8.5	37.0	50.6
Ir–1 Re	16.5	37.0	43.0
Ir–1.98 Re	20.0	42.7	51.1
Ir–3.96 Re	16.8	51.2	30.3
Ir–8 Re	18.0	68.8	31.0

[a]Tested in vacuum at a crosshead speed of 0.05 to 0.2 in./min; all specimens annealed 1 hr at 1500°C in vacuum before testing.

Air Oxidation

A study of the air oxidation of Ir–0.65% Hf, Ir–10% Ru, and Ir–8% Re alloys has continued. The sheet specimens were oxidized in the furnace at an air flow rate of 100 liters/hr at 770 and 870°C. At present, the oxidation runs have logged 1500 hr. The results continue to indicate that the oxidation rate of Ir–8% Re is more than an order of magnitude higher than the other two alloys.

Thermomechanical Effects on Iridium-Tungsten Alloys

C. T. Liu

Sheets of Ir–0.1% W and Ir–0.5% W alloys (prepared from OEP iridium powder) warm rolled at 950°C were vacuum annealed 1 hr between 800 and 1600°C for microstructural examination and determination of recrystallization temperatures. The as-rolled sheets showed essentially a fibrous structure; however, a very few recrystallized grains were observed in Ir–0.1% W sheet. The recrystallization temperatures for the two alloys are presented in Table 9 together with those for other iridium-tungsten alloys reported previously.[3] The data clearly indicate that

[3] R. G. Donnelly, Isotopic Power Materials Development Progress Report for August 1973, ORNL-TM-4383.

Table 9. Effect of 1-hr Heat Treatment on the Recrystallization Temperatures of Iridium-Tungsten Alloys

Tungsten Content (wt %)	Recrystallization Temperature, °C		
	0%	50%	100%
0 (EBP-21)[a]	800	870	950
0.09 (EBP-19)[a]	800	880	1000
0.1	850	960	1030
0.3 (WC-4)[a]	870	970	1070
0.5	1000	1100	1200
1.0	1100	1200	1300
1.92	1200	1300	1400

[a] Ingot or sheet number used by the Iridium Fabrication Program.

recrystallization temperatures increase with tungsten content. The recrystallization temperature of Ir–0.5% W is higher by 130°C than that of Ir–0.3% W currently used for MHW flight hardware.

Evaluation of Impact Behavior of PICS

C. T. Liu and H. Inouye

The post-impact containment shells (PICS) produced by ORNL/MRC often show the fingerprint-type cracks on the impact face when impacted at 1370°C at a velocity of about 300 fps. In some cases, these cracks lead to breach of the containment shell. Postmortem analyses revealed that the fracture morphology of these cracks was almost completely intergranular, indicating the weakness of the grain boundaries. The purpose of this work is to study the PICS material and its correlation with fingerprint-type cracking. The task emphasizes a fix, if possible.

It is not clear at present how the fingerprint-type cracks develop during high-temperature high-velocity impact, so we attempted to attack this problem from various approaches. Review of the progress reports from LASL and GE indicates that PICS fabricated from EI sheets resist fingerprinting better than those fabricated from ORNL-produced sheets. Thus, we first attempted to evaluate what differences in chemical make-up and mechanical properties exist between EI and ORNL materials. The sheet specimens fractured by tensile tests at various temperatures were examined by binocular and optical microscopes. Their fracture modes are presented in Table 10 together with tensile data; some conclusions can be drawn from the comparison.

1. Iridium and iridium alloys exhibited completely ductile rupture at 1093 to 1370°C (data are not presented in Table 10). In fact, most of them necked down to a knife-edge before final separation.

2. The iridium and iridium alloy sheets showed transgranular fracture (TF), grain-boundary separation (G-B-S), or a mixture of both at or below 760°C.

3. Comparison of the fracture modes of the sheets containing about 0.3% W indicates that EI material (S-74, EI-114-C) is more resistant to

Table 10. Tensile Properties[a] of Iridium and Iridium Alloy Sheets

Material (wt %)	Elongation (%)	Strength, ksi Yield	Strength, ksi Tensile	Fracture Mode[b]
		Room Temperature		
S-74[c]	9.7	16.1	63.2	Mixture of G-B-S and TF
EI-114-C[c]	13.5	13.3	63.2	Mainly G-B-S
EBP-21[d]	14.1	7.2	48.0	G-B-S
WD-1[e]	14.2	13.0	61.3	Mainly G-B-S
WC-4[e]	12.1	13.4	55.7	Mainly G-B-S
WE-3[e]	12.4	13.1	60.4	Mainly G-B-S
Ir–1 W[f]	6.8	29.1	56.0	Mainly G-B-S
Ir–1.92 W[f] (Ir-15)	8.3	36.7	70.3	G-B-S
Ir–1.92 W[g] (Ir-38)	8.4	32.8	64.0	G-B-S
Ir–3.84 W[g]	4.0	51.7	64.0	G-B-S
Ir–1 Re[h]	6.6	25.5	48.0	Mixture of G-B-S and TF
Ir–1.98 Re[h] (Ir-14)	8.9	26.0	67.6	Mainly G-B-S
Ir–1.98 Re[i] (Ir-45)	11.2	26.1	71.0	Mainly G-B-S
Ir–1.98 Re–0.4 W[f]				Mixture of G-B-S and TF
Ir–3.96 Re[g]	6.4	32.1	60.6	Mainly G-B-S
		500°C		
S-74[c]	17.8	14.0	76.4	Mixture of G-B-S and TF
Ir–1 W[f]	13.8	26.0	63.0	Mixture of TF and G-B-S
Ir–2 W[f] (Ir-15)	21.5	28.0	93.3	Mainly G-B-S
Ir–1.98 Re[h] (Ir-14)	13.7	26.2	62.5	Mixture of G-B-S and TF
Ir–1.98 Re–0.4 W[f]	12.3	32.1	68.0	Mainly TF
		650°C		
EI-114-C[c]	37.6	13.6	74.2	Mixture of G-B-S and TF
WD-1[e]	32.2	10.7	70.4	Mainly G-B-S
		760°C		
S-74[c]	25.0	16.0	60.5	TF
EI-114-C[c]	38.6	15.4	64.0	Mainly TF
EBP-21[d]	38.4	8.2	56.9	Mixture of G-B-S and TF
WD-1[e]	42.5	9.3	58.7	Mainly TF
WC-4[e]	32.5	7.5	58.1	Mainly TF
WE-3[e]	34.0	11.0	65.6	Mixture of G-B-S and TF
Ir–1 W[f]	24.4	23.6	58.0	TF
Ir–1.92 W[f] (Ir-15)	30.0	22.2	84.2	Mixture of G-B-S and TF
Ir–1.92 W[g] (Ir-38)	29.1	21.2	79.8	Mainly G-B-S
Ir–3.84 W[g]	10.6	30.0	57.3	Mainly G-B-S
Ir–1 Re[h]	20.0	22.0	50.0	TF
Ir–1.98 Re[h] (Ir-14)	28.0	19.3	67.3	Mainly TF
Ir–1.98 Re[i] (Ir-45)	32.1	14.2	74.9	Mixture of TF and G-B-S
Ir–1.98 Re–0.4 W[f]	21.8	21.0	58.5	TF
Ir–3.96 Re[g]	20.2	23.1	70.2	Mixture of G-B-S and TF

[a]Tested at a crosshead speed of 0.05 to 0.2 in./min; all specimens annealed 1 hr at 1500°C before testing.

[b]G-B-S = grain-boundary separation; TF = transgranular fracture.

[c]EI material containing about 0.3% W.

[d]ORNL material.

[e]ORNL material containing 0.3% W.

[f]Alloys prepared from EI material.

[g]Alloys prepared from OEP powder at ORNL.

[h]Alloys prepared from Matthey-Bishop powder at ORNL.

[i]Alloys prepared from recycling powder at ORNL.

G-B-S than the ORNL sheets (WD-1, WC-4, WE-3). In other words, the grain boundaries are less embrittled in the EI material.

4. The EI material is stronger than the ORNL material at all temperatures.

5. There is no reasonable correlation between the tensile elongation and the fracture mode.

6. The fracture behavior of Ir-W and Ir-Re alloys is sensitive to the starting material used to prepare the alloys. For instance, the three Ir–1.98% Re sheets prepared from EI stock (containing 0.4% W), Matthey-Bishop powder and recycled iridium powder, showed, respectively, TF, mainly TF, and a mixture of TF and G-B-S at 760°C. Also, the two Ir–1.92% W alloys showed a mixture of G-B-S and TF, and mainly G-B-S at 760°C when EI stock and OEP material are used as starting material, respectively.

7. The material most resistant to the G-B-S is Ir–1.98% Re–0.4% W which showed mainly TF at a temperature as low as 500°C. Note that this alloy was prepared by alloying rhenium with EI material, S-74.

It appears from these results that the fracture characteristics are governed by the impurities in iridium alloys, and their effects are not canceled by alloying and/or remelting.

To determine the impurity content in various materials, the spark-source mass-spectrographic (SSMS) method was used to analyze the chemical content of tensile specimens fractured at room temperature. Table 11 gives the results of both bulk concentration (corresponding to long-time exposure of fracture surface to ionizing beam) and surface concentrations (corresponding to various short-time exposures). The shortest exposure gives the possible concentration at grain boundaries. The range indicated by the GB column corresponds to the impurity gradient near the grain boundary. The data indicate that the ORNL material has a purity higher than EI material. The impurities whose average concentrations are significantly higher in EI than ORNL materials are listed in Table 12. The impurities can be characterized into two categories – elements such as Th, Ta, Fe, and Al, whose concentration at the GB is higher than bulk value by two to four orders of magnitude, and secondly, elements such as Rh, Ni, and Cu, whose grain boundary concentration is

Table 11. Chemical Analyses[a] of Iridium and Iridium Alloy Sheet Specimens[b] Fractured at Room Temperature

Element	EI-870-M[c]		EI-114-C[d]		S-74[e]		Ir-1.98 Re-0.4 W[f]		EBP-21[g]		WC-4[g]		WD-1[g]		WE-3[g]		Ir-1.92 W[g]	
	Bulk[h]	GB[i]	Bulk[h]	GB[i]	Bulk[h]	GB[i]	Bulk[h]	GB[i]	Bulk[h]	GB[i]	Bulk[h]	GB[i]	Bulk[h]	GB[i]	Bulk[h]	GB[i]	Bulk[h]	GB[i]
Al	20	50–1000	60	1000–10,000	Not determined	10–70	2	40–70	1	50–200	2	50–150	Not Determined	10–30	Not Determined	20	1	20–80
B	0.2	<10	0.2	20–70		30	0.5	10	0.2	5–20	0.2	10		<10–30		5–10	0.2	5–20
Ca	6	20–100	2	200–800		50–200	1	50	6	30–200	6	10–30		10–100		20–100	6	50
Co	11		0.3				20		0.3		6						6	
Cr	10	100–2000	3	300–1500		<20	8	<20	3	50–200	30	<20		<50–200		20–100	3	<20–50
Cu	30	100–300	50	100–400		<20	3	<20	10	<20–200	3	<20		<20		30–100	3	<20
Fe	150	100–4000	15	1000–3000		200–600	25	200–500	15	200–2000								
Hf	<0.4		<0.4				<2		<0.4		<0.4						<0.4	
K	0.6	20–150	2	800–8000		30–70	3	70	2	100–1000	6	50–200		10–500		100–400	6	50–250
Mg	0.4		0.4				2		0.4		0.4						<0.4	
Mn	3		1				<1		0.3		0.3						0.3	
Mo	3		1				70		3		3						10	<50–100
Ni	10	20–200	10	20–50		<50	10	<50–200	1	<50	1	<20		<20		<50	1	<20
Os	<0.4		<0.4				<0.4		<0.4		<0.4						<0.4	
P	0.2		<0.1				<1		<0.1		0.3						0.1	
Pd	6		0.6				<2		<0.2		0.2						<0.2	
Pt	1		1				<20		1		1						1	
Re	<0.2		<0.2				>1%	~2%	<0.2		<0.2						6	
Rh	50		50				30		20		2						2	
Ru	2		0.5				300		20		20						20	
Si	3	100–500	10	500–2000		50–90	30	200–400	10	200–1000	100	200–600		50–1000		200	30	200–600
Sn	6		0.6						<0.2		<0.2						<0.2	
Ta	30	80–3000	3	2000–5000		<50	50	<50	3	<100	3	<50		20–300		<50	3	<100
Th	10	2000–20,000	1	<50–5000		1000–10,000	80	<50–2000	<0.1	<50–800	<0.1	<100		<50		<50	<0.1	<100
Ti	1	<50	1	100–600			80		1	<50	≤3						≤3	<50
V	3		1	<10–50			10		3		3						3	
W	4000	~4000	~1%			4000	4000	4000	10	<1000	4000	4000–15,000		3000		3500	<1%	~2%
Zn	0.1	<50–300	0.1	100–600		<20	2	<20	0.1	<20	0.1	<20		<20		20	<0.1	<20
Zr	0.3		0.1				50		0.1		0.3						1	
Br	0.3		<0.1				2		0.1		<0.1						<0.1	
S	3	50–500	1	800–8000		<50–200	40	<50	3	600–3000	1	<50		<50–500		<50–400	1	<50–1000
Cl		50–300		1000–10,000		100–300	5	100–350		200–1000		<50–200		50–1000		100–500		200–600

[a]Analysis in parts per million by SSMS method. [b]Annealed 1 hr at 1500°C prior to tensile testing. [c]PICS produced from EI material, Lot No. 52.
[d]Sheet produced by EI. [e]1/8 in. plate received from EI and fabricated to sheet at ORNL. [f]Prepared from EI material S-74.
[g]ORNL material prepared from OEP powder. [h]Bulk concentration obtained from long-time exposure of fracture surface to ionized beam.
[i]Surface concentration obtained from various short-time exposures of fracture surface to ionized beam.

Table 12. Average Concentration[a] of Impurity in Sheets Produced at ORNL and EI

Element	EI[b]		ORNL[c]	
	G.B.	Bulk	G.B.	Bulk
Al	500–6000	40	30–100	2
Cr	200–1600	7	30–140	16
Cu	100–350	40	30–150	6
Fe	500–3500	85	80–750	15
Ni	20–130	10	< 30	1
Rh		50		11
Ta	1050–4000	17	20–120	3
Th	1000–13,000	6	< 50–150	< 0.1
Zn	70–450	0.1	< 20	0.1

[a]Analysis in parts per million.

[b]Average content in EI-870-M and EI-114-C sheets produced by EI.

[c]Average content in EBP-21, WC-4, WD-1, WE-3 sheets produced at ORNL.

less significantly different from bulk values. As indicated in Table 10, iridium alloys prepared from EI stock resist G-B-S better than the ORNL sheets prepared from OEP powder. It is possible that the impurity elements listed in Table 12 contribute to this difference. Thus, we are planning to prepare iridium or Ir–0.3% W alloys containing these impurities for studying their fracture modes at various test temperatures.

Iridium and iridium alloys showed intergranular fracture and low ductility at low test temperatures (see Table 10), indicating the possibility that fingerprints result from deformation at a temperature considerably lower than the impact temperature. This may occur during impact of fuel source assembly (FSA); for instance, PICS are subject to rebounding-type impacts or severe thermal gradients on the impact surface where graphite impact shell (GIS) is crushed during the primary impact. To simulate the heat-treatment conditions of an FSA, sheet specimens of EI-114-C, WC-3, and EBP-21 were contacted with ATJ

graphite on one side and annealed 18 hr at 1500°C in vacuum. The heat-treated specimens were strained approximately 14% at 1370°C (to simulate the deformation of impact) and then tensile tested at 760 or 500°C to simulate stresses and strains induced by secondary impacts all those produced by severe thermal gradients. The results are presented in Table 13. Although the ductility was reduced considerably by the prestrain at 1370°C (compared with the data without prestrain in Table 10), the specimens still have a ductility of 20 to 30% at 500 to 760°C. Only a few surface cracks were observed at 760°C in the areas adjacent to the fracture section; however, the remainder of the specimen was free from such cracks. There was no preferential location of surface cracks on the surface contacted with graphite.

Table 13. Tensile Properties of Iridium and Ir–0.3% W Sheet Specimens[a] Prestrained about 14% at 1370°C and Then Strained to Fracture at 760 or 500°C

Heat Number	Test Temperature (°C)	Tensile Strength (ksi)	Elongation (%)	Surface Crack[b]	Fracture Mode[c]
EI-114-C	760	56.0	27.3	A few surface cracks adjacent to FA	TF
EI-114-C	500	69.2	19.6	No surface cracks	Mainly G-B-S
WC-3	760	54.4	28.5	A few surface cracks adjacent to FA	Mainly TF
EBP-21	760	43.8	18.5	A few surface cracks adjacent to FA	Mixture of TF (major) and G-B-S (minor)

[a]Specimens contacted with ATJ graphite on one side, annealed 18 hr at 1500°C in vacuum, tested at a crosshead speed of 0.1 to 0.2 in./min.

[b]FA = fracture area.

[c]TF = transgranular fracture; G-B-S = grain boundary separation.

Ruthenium Characterization and Fabrication Development

H. Inouye

An exploratory investigation of the properties of pure ruthenium commenced in December to determine its potential as a fuel cladding for isotopic fuels. The principal attributes, the expected problems, and the initial consolidation of powders to an electron-beam-melted button have been described.[4,5] The hot rolling characteristics of a 72-g rectangular button 5/16 × 1 1/8 × 1 7/16 in. sealed in a molybdenum frame and cover plates will be determined in late February or early March.

Platinum-Rhodium-Tungsten Alloys

H. Inouye

The development work on Pt-Rh-W alloys to date continues to show adequate fabrication characteristics and attractive high-temperature properties in certain heats, but in other heats we have encountered severe ingot cracking during hot rolling. In all cases, the alloy is characterized by the occurrence of a minimum in the ductility between 1000 and 1100°C. In some heats the ductility minimum is scarcely detectable, but in others is quite severe. Although a state of "technology ready" has not been demonstrated, this stage could be soon attained if the task had a higher priority than it does relative to the Iridium Fabrication Program activities and suitable melting stock were available as evidenced by the following recent results.

The effect of the melting process on the fabricability and the tensile properties of several heats of Pt-3008 (Pt–30% Rh–8% W) was determined. The first series consisted of three heats using the same melting stock known to have higher-than-normal levels of boron and

---

[4]R. G. Donnelly, Isotopic Power Materials Development Progress Report for December 1973, ORNL-TM-4534 (to be published).

[5]R. G. Donnelly, Isotopic Power Materials Development Progress Report for January 1974, ORNL-TM-4535 (to be published).

osmium. Heat Pt-4MR was formulated by arc melting together the "as-received" platinum, rhodium, and tungsten; heat Pt-4XR was prepared by arc melting the previously electron-beam-melted components, and heat Pt-5D was prepared by electron-beam-melting scrap from heats Pt-4MR and Pt-4XR. All ingots developed surface cracks transverse to the hot rolling direction, the severity of which decreased in the order 4MR, 4XR, and 5D. The tensile properties of sheet from these heats are compared in Table 14. Although the specimen prepared from the electron-beam-melted ingot reflects higher ductility at 1093 and 1316°C, the severe ductility minimum persists regardless of the melting process.

The second series of Pt-3008 consisted of two heats prepared from melting stock with low boron and no osmium. The first ingot in this series (heat Pt-4N) was arc melted in the manner of heat Pt-4XR and the second ingot (heat Pt-4E) was electron-beam-melted scrap from heats

Table 14. Tensile Properties[a] of Pt-3008 Sheet Prepared from Melting Stock Containing High Boron and Osmium

Heat Number[b]	Test Temperature (°C)	Strength, ksi		Elongation (%)
		Ultimate	0.2% Yield	
Pt-4MR	Room	132.7	63.4	38.6
Pt-4XR	Room	128.8	57.6	44.4
Pt-5D	Room	124.0	55.0	32.6
Pt-4MR	760	95.8	40.5	26.2
Pt-4XR	760	69.5	40.1	11.4
Pt-5D	760	79.0	41.6	15.6
Pt-4MR	1093	33.0	28.3	4.0
Pt-4XR	1093	32.8	26.4	4.8
Pt-5D	1093	37.4	26.0	8.0
Pt-4MR	1316	19.4	17.2	22.4
Pt-4XR	1316	19.4	18.0	39.8
Pt-5D	1316	18.3	18.3	48.8

[a]Cold rolled 50%, vacuum annealed 1 hr at 1200°C. Gage dimensions: 0.020 × 0.125 × 0.500 in; strain rate 0.2 min^{-1}.

[b]Heat 4MR prepared by arc melting as-received melting stock; heat 4XR prepared by arc melting electron-beam melted platinum and rhodium; heat 5D prepared by electron-beam-melting above arc-melted scrap.

similar to heat Pt-4N. Surface cracking was not encountered, and a high-quality sheet was produced from both ingots. The tensile properties are compared in Table 15. As previously noted, increased ductility characterized the sheet produced from the electron-beam melt; however, the improvement near the ductility minimum (i.e., 1093°C) again was modest.

Table 15. Tensile Properties[a] of Pt-3008 Sheet Prepared from Melting Stock Containing Low Boron and Osmium

Heat Number	Test Temperature (°C)	Strength, ksi		Elongation (%)
		Ultimate	0.2% Yield	
Pt-4N[b]	Room	105.0	55.1	18.4
Pt-5E[c]	Room	124.4	52.3	39.4
Pt-4N	760	81.4	26.6	38.4
Pt-5E	760	75.9	26.5	34.8
Pt-4N	1093	40.5	22.7	15.2
Pt-5E	1093	38.5	19.6	19.0
Pt-4N	1316	21.0	16.1	33.4
Pt-5E	1316	20.0	15.9	68.8

[a]Cold rolled 50%, vacuum annealed 1 hr at 1200°C. Gage dimensions: 0.020 × 0.125 × 0.500 in; strain rate 0.2 min^{-1}.

[b]Arc melted using electron-melted platinum and rhodium.

[c]Electron-beam-melted scrap from heats similar to Pt-4N.

The above data clearly indicate that the fabricability and the tensile properties are principally determined by the impurities in the melting stock. These impurities appear to become less noxious (presumably by some purification) on remelting, but still persist regardless of the melting process. Because improvement in the alloy properties was modest after electron beam melting, it appears that the harmful impurities are not highly volatile. Both boron and osmium fit these requirements.

Auger, SEM, SSMS, and vacuum fusion analyses were used to identify the probable impurities responsible for the cracking problem and the

cause of the ductility minimum. Auger analyses showed 20 at. % B, higher than nominal rhodium, no osmium, and very low tungsten on the fractured surface of as-cast Pt–4MR! Complete intergranular fracture and the presence of bubbles or voids on the grain surfaces were shown by SEM micrographs. The grain boundary impurities suggest that a low-melting-point ternary boride containing Pt-Rh-B is the reason for the poor mechanical properties and the lack of fabricability. Osmium was not implicated by these data.

Spark-source mass-spectrometry analyses of the fractured surfaces of selected tensile specimens tested at 1093°C were obtained in an attempt to correlate the ductility minimum with the boron content. The results in Table 16 show the clear dependence of the ductility on the boron content at the fracture surface. The ductility showed no dependence on Ca, Co, Fe, K, Mg, Mo, Na, Nb, Ta, or O content.

Table 16. The Dependence of the High-Temperature Ductility of Pt-Rh-W Alloys on the Boron Content[a]

Heat Number	Nominal Composition (wt %)	Boron Content on Fracture Surface (ppm)	Elongation at 1093°C (%)
Pt-1ER	Pt–26 Rh–8 W	0.2	34.2[a]
Pt-5E	Pt–30 Rh–8 W	10	19.0
Pt-1M	Pt–26 Rh–8 W	30	9.7
Pt-4XR	Pt–30 Rh–8 W	100	4.8

[a]Test at 1000°C.

CURIUM-244 FUEL DEVELOPMENT

Compatibility Testing

J. R. DiStefano

FY-1973 Compatibility Matrix

Compatibility test capsules listed in Table 17 were transferred to the High Radiation Level Examination Laboratory for examination. However, operations at HRLEL have been interrupted for the past six weeks to allow for cell cleanup and new equipment installation. Examination of couples from these tests is expected to begin by late March.

Table 17. $^{244}Cm_2O_3$ Compatibility Test Conditions

Set Number	Test Materials and Conditions
1	900°C; 5000 hr; helium atmosphere; Ir, C, Pt, Hf–1% Pt–0.5% Pd, Hastelloy C-276, Haynes alloy 25, Haynes alloy 188, ThO_2, Pt–20% Rh, and Pt–26% Rh–8% W
2	900°C; 5000 hr; graphite, helium atmosphere; Ir, Pt, Hf–1% Pt–0.5% Pd, Hastelloy C-276, Haynes alloy 25, Haynes alloy 188, ThO_2, Pt–20% Rh, and Pt–26% Rh–8% W
7	1400°C; 5000 hr; graphite, helium atmosphere; Ir, C, Mo, Mo–46% Re, Ta, T-111, W, and W–26% Re
8	1400°C; 5000 hr; dynamic vacuum; Ir, Mo, Mo–46% Re, Ta, T-111, W, and W–26% Re
9	1400°C; 5000 hr; helium atmosphere; Ir, Mo, Mo–46% Re, Ta, T-111, W, and W–26% Re
10	1400°C; 5000 hr; graphite, dynamic vacuum; Ir, C, Mo, Mo–46% Re, Ta, T-111, W, and W-26% Re

FY-1974 Compatibility Matrix

A test system that will incorporate mechanical properties specimens for evaluation with $^{244}Cm_2O_3$ has been designed (Fig. 1). A specimen package consisting of four sheet tensile specimens and two fuel frames containing two rectangular $^{244}Cm_2O_3$ samples is held together by two nuts and bolts made from the material being evaluated. Although the

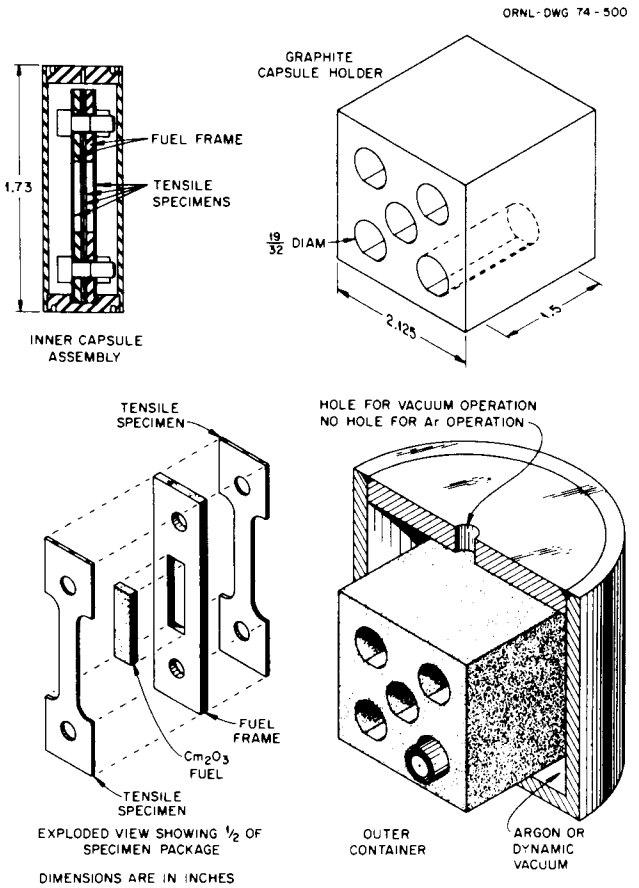

Fig. 1. $^{244}Cm_2O_3$ Mechanical Properties Compatibility Test System.

$^{244}Cm_2O_3$ fuel pellet should be held in contact with the tensile specimens by the nuts and bolts, we will orient the specimen package so that at least a gravity force is maintained. The specimen package fits into a slot in the bottom end plug that will keep it from turning, and the end plug will be indexed with respect to a flat machined on the outside surface of the inner capsule that will allow it to lock into position in the graphite holder. Test conditions selected are as indicated below:

5000 hr – 900°C Argon-Graphite	5000 hr – 1100°C Vacuum-Graphite	10,000 hr – 1400°C Vacuum-Graphite
Pt-3008/TZM*	Pt-3008	W–26% Re
Haynes alloy 188/ Ta–10% W*	Mo–46% Re	Mo–46% Re
Mo–46% Re	Ta–10% W	Ta–10% W
TZM		
Ta–10% W		

*Outer sealed container surrounding vented inner capsule.

Procurement and fabrication of test components are now under way. The alloys, Haynes 188, Ta–10% W, TZM, and W–26% Re, were obtained from commercial sources. The alloys Mo–46% Re and Pt-3008 were not available commercially and material was prepared by melting, casting, and sheet rolling procedures. Procedures to form and weld cylindrical tubes from sheet were developed for these materials. All capsule bodies, end plugs, fuel frames, and nuts and bolts have been received.

Tensile specimens of all the materials except W–26% Re are to be die punched from sheet at room temperature. The W–26% Re alloy tends to develop edge cracks when sheared; therefore, tensile specimens of this material were prepared by machining and grinding operations.

In addition to the mechanical properties tests, two ceramic materials, ZrO_2 and Si_3N_4, will be tested with $^{244}Cm_2O_3$ for 5000 hr at 900°C. Capsules will be vented to an argon atmosphere and will be in contact with graphite. The ZrO_2 test specimen is rigidized felt, and the container material is Y_2O_3 stabilized ZrO_2. Three disk specimens of Si_3N_4 have been supplied by Gulf General Atomic. Containers have not yet been fabricated, since Si_3N_4 is not available in capsule form. Molybdenum, which has excellent compatibility with $^{244}Cm_2O_3$ at 900°C, is also reported to have good compatibility with SiN_4 and will probably be used as the container material.

Graphite capsule holders and Haynes alloy 25 (900°C) and Ta (1100 and 1400°C) outer containers for these tests have been received. The Haynes alloy 25 outer containers will be subjected to about 5 atm pressure over the 10,000-hr test life. These containers were machined from heavy-wall pipe and 0.25-in.-thick plate is being used for the end caps. Inspection of the bottom end plug welds indicates minimum penetration of 0.100 in., which should be adequate.

INTERNAL DISTRIBUTION

1. D. N. Braski
2. J. E. Cunningham
3. J. H. DeVan
4. J. R. DiStefano
5–9. R. G. Donnelly
10. J. I. Federer
11. M. R. Hill
12. H. Inouye
13. R. W. Knight
14. E. Lamb
15. C. T. Liu
16. C. L. Ottinger
17. R. E. McDonald
18. A. J. Moorhead
19. P. Patriarca
20. H. Postma
21. M. E. Ramsey
22. A. C. Schaffhauser
23. D. B. Trauger
24. T. N. Washburn
25. J. R. Weir, Jr.
26–27. Central Research Library
28. Document Reference Section
29–31. Laboratory Records
32. Laboratory Records, ORNL-RC
33. ORNL Patent Office

EXTERNAL DISTRIBUTION

34. M. Ault, Lewis Research Center
35–37. R. D. Baker, Los Alamos Scientific Laboratory
38. R. Brouns, Langley Research Center, NASA
39. R. T. Carpenter, Division of Space Nuclear Systems, AEC
40. W. T. Cave, Monsanto Research Corporation
41. G. R. Crane, Andrews AFB
42. G. Deutsch, NASA Headquarters
43. G. P. Dix, Division of Space Nuclear Systems, AEC
44. R. DuVal, San Francisco Operations Office
45. N. Elsner, Gulf Energy and Environmental Systems
46. J. Epstein, Goddard Space Flight Center, NASA
47. R. Fischell, Johns Hopkins University
48. D. S. Gabriel, Division of Space Nuclear Systems, AEC
49. N. Goldenberg, Division of Space Nuclear Systems, AEC
50. E. F. Hampl, Minnesota Mining and Manufacturing Company
51. W. S. Hollman, Division of Applied Technology, AEC
52. R. G. Ivanoff, Jet Propulsion Laboratory
53. H. Jaffe, Division of Space Nuclear Systems, AEC
54. E. W. Johnson, Monsanto Research Corporation
55. G. W. Johnson, Division of Applied Technology, AEC
56. I. Jones, TRW Systems
57. R. J. Katucki, General Electric Company
58. D. P. Kelly, Monsanto Research Corporation
59. T. B. Kerr, NASA Headquarters
60. G. Linkous, Isotopes, Inc.
61. J. J. Lombardo, Division of Space Nuclear Systems, AEC
62. J. N. Maddox, Division of Biomedical and Environmental Research, AEC

63. J. McDonald, Sandia Laboratories
64. R.N.R. Mulford, Los Alamos Scientific Laboratory
65. H. Nelson, Ames Research Center, NASA
66. T. A. Nemzek, Division of Reactor Research and Development, AEC
67. G. A. Newby, Division of Space Nuclear Systems, AEC
68. A. Noonan, Kirtland AFB
69. D. Ofte, Albuquerque Area Office, AEC
70. W. Pardue, Battelle Memorial Institute
71. T. E. Redding, Manned Spacecraft Center
72. R. W. Shivers, Division of Applied Technology, AEC
73. J. M. Simmons, Division of Reactor Research and Development, AEC
74. A. A. Solomon, Argonne National Laboratory
75. M. D. Starr, Naval Facilities Engineering Command
76. C. O. Tarr, Division of Space Nuclear Systems, AEC
77. V. Truscello, Jet Propulsion Laboratory
78. D. R. Turno, Savannah River Laboratory
79. E. J. Wahlquist, Division of Space Nuclear Systems, AEC
80. R. L. Wainwright, Dayton Area Office, AEC
81. D. Watrous, Donald W. Douglas Laboratories
82. A. Wilbur, Ames Research Center, NASA
83. Directorate of Nuclear Safety, Kirtland AFB
84. Research and Technical Support Division, ORO
85–86. Technical Information Center, OR